CrossMark
click for updates

View Article Online
View Journal

Nanoscale

Accepted Manuscript

This article can be cited before page numbers have been issued, to do this please use: A. Santos, C. S. Law, T. Pereira and D. Losic, *Nanoscale*, 2016, DOI: 10.1039/C6NR01068G.

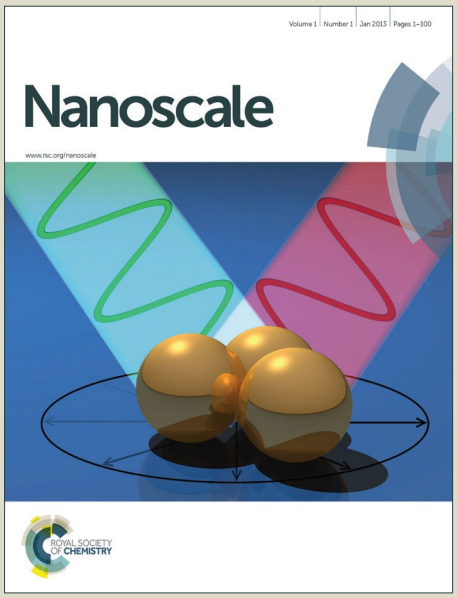

This is an *Accepted Manuscript*, which has been through the Royal Society of Chemistry peer review process and has been accepted for publication.

Accepted Manuscripts are published online shortly after acceptance, before technical editing, formatting and proof reading. Using this free service, authors can make their results available to the community, in citable form, before we publish the edited article. We will replace this *Accepted Manuscript* with the edited and formatted *Advance Article* as soon as it is available.

You can find more information about *Accepted Manuscripts* in the Information for Authors.

Please note that technical editing may introduce minor changes to the text and/or graphics, which may alter content. The journal's standard Terms & Conditions and the Ethical guidelines still apply. In no event shall the Royal Society of Chemistry be held responsible for any errors or omissions in this *Accepted Manuscript* or any consequences arising from the use of any information it contains.

ROYAL SOCIETY OF CHEMISTRY

www.rsc.org/nanoscale

View Article Online
DOI: 10.1039/C6NR01068G

Nanoscale

RSCPublishing

PAPER

Published on 14 March 2016. Downloaded by University of California - San Diego on 14/03/2016 13:36:14.

Cite this: DOI: 10.1039/xoxxoooooox

Nanoporous Hard Data: Optical Encoding of Information within Nanoporous Anodic Alumina Photonic Crystals

Abel Santos[1*], Cheryl Suwen Law[1], Taj Pereira[1] and Dusan Losic[1*]

Received ooth August 2016,
Accepted ooth August 2016

DOI: 10.1039/xoxxoooooox

www.rsc.org/

Herein, we present a method for storing binary data within the spectral signature of nanoporous anodic alumina photonic crystals. A rationally designed multi-sinusoidal anodisation approach makes it possible to engineer the photonic stop band of nanoporous anodic alumina with precision. As a result, the transmission spectrum of these photonic nanostructures can be engineered to feature well-resolved and selectively positioned characteristic peaks across the UV-visible spectrum. Using this property, we implement a 8-bit binary code and assess the versatility and capability of this system by a series of experiments aiming to encode different information within nanoporous anodic alumina photonic crystals. The obtained results reveal that the proposed nanosized platform is robust, chemically stable, versatile and has a set of unique properties for data storage, opening new opportunities for developing advanced nanophotonic tools for a broad range of applications, including sensing, photonic tagging, self-reporting drug releasing systems and secure encoding of information.

Introduction

Many living organisms store information within hard structures of their bodies such as teeth, skeleton and bones.[1] For instance, seal teeth, sharks vertebrae, annual rings in trees or coral structures contain important ecological and environmental information encoded as variations of density and/or composition.[2] The information contained within these hard data structures can be readily used to cast light on some critical questions affecting our flora, fauna and environment (e.g. reconstruction of historical climate-growth associations, impact of human activity over natural habitats, etc.). In a similar manner, from the early days using rocks, stones and paper as storage platforms to the modern days in the form of magnetic tapes and memories, floppy and compact discs, hard drives and virtual e-clouds, synthetic hard data platforms have been long used by mankind to store information. Physical platforms used for this purpose, however, present several drawbacks. For example, magnetic and optical discs platforms used to store information are big in size, need to be maintained regularly and are prone to decay with time and use.

In recent years, scientists have explored, developed and demonstrated alternative synthetic platforms aimed to store data in a secure and stable manner, within nanoscale platforms. So far, various encoding systems have been proposed, including fluorescent and DNA molecules, metal rods, quantum dots and photonic crystals.[3-9] Among them, porous silicon-based photonic crystals have been envisaged as an outstanding and versatile platform for storing encoded information.[10] This concept, pioneered by Berger et al. and fully developed by Sailor and co-workers, is based on the generation of porous silicon (pSi) photonic crystals prepared by electrochemical etching of silicon substrates through complex etching current profiles.[10,11-14] pSi photonic crystals produced by this approach feature well-resolved reflection peaks, the position and intensity of which across the UV-visible spectrum correspond to the Fourier transform of the composite current etching waveform used to create the pSi photonic crystal. Sailor and co-workers demonstrated that the position and amplitude of these characteristic reflection peaks can be precisely tuned by the current etching profile, enabling a binary encoding system with ON(1)/OFF(0) states. Regardless of the advantages and versatility offered by pSi photonic crystals, it is worthwhile stressing that pSi oxidises when exposed to air or aqueous solutions and degrades under acidic or basic media conditions unless passivated via chemical functionalisation or carbonisation.[15-17] As a result of these chemical and physical changes, the optical information contained within pSi photonic crystals is unstable, hindering the broad applicability of this optical encoding platform.

Nanoporous anodic alumina (NAA) produced by anodisation (i.e. electrochemical oxidation) of aluminium features superior properties than those of pSi in terms of mechanical, thermal and chemical stability, fully controllable and versatile nanopore geometry and can be produced by an industrially-scalable and cost-competitive process, which has been utilised by metal finishing industry for more than a century.[18-22] In spite of these advantageous characteristics, the use of NAA as a platform for developing photonic structures has been hindered due to its intrinsic limitations. Anodisation of aluminium under mild conditions is an electrochemical process that relies upon the diffusion of ionic species (i.e. Al^{3+}, O^{2-}, OH^-, etc.) across the oxide barrier layer located at the bottom of the nanopores in the oxide film. This oxide barrier layer, which acts

Nanoscale Accepted Manuscript

PAPER View Article Online DOI: 10.1039/C6NR01068G Nanoscale

Published on 14 March 2016. Downloaded by University of California - San Diego on 14/03/2016 13:36:14.

as an electric/ionic insulator, impedes the direct translation of current density/voltage modifications into porosity/nanopore geometry changes (i.e. parameter used to engineer the effective refractive index of NAA in depth) as the flow of ionic species undergoes a recovery stage when the driving force (i.e. voltage or current density) is modified during anodisation.[23-25] Lee and co-workers pioneered a set of electrochemical approaches aimed to engineer the structure of NAA in depth. These seminal works paved the way for creating NAA-based photonic crystals with precisely engineered optical properties.[26-30] In recent years, we and others have further explored advanced structural engineering approaches aiming to develop a broad range of NAA-based photonic structures, including distributed Bragg reflectors, rugate filters and microcavities.[31-57] In a recent study, we developed an innovative and rationally designed anodisation method, so-called sinusoidal pulse anodisation, aiming to engineer the effective refractive index of NAA in a sinusoidal manner with precision.[58] Sinusoidal pulse anodisation under the conditions used in our study enables the direct translation of sinusoidal anodisation profiles under mild conditions into sinusoidal modulations of the effective refractive index of NAA in depth.

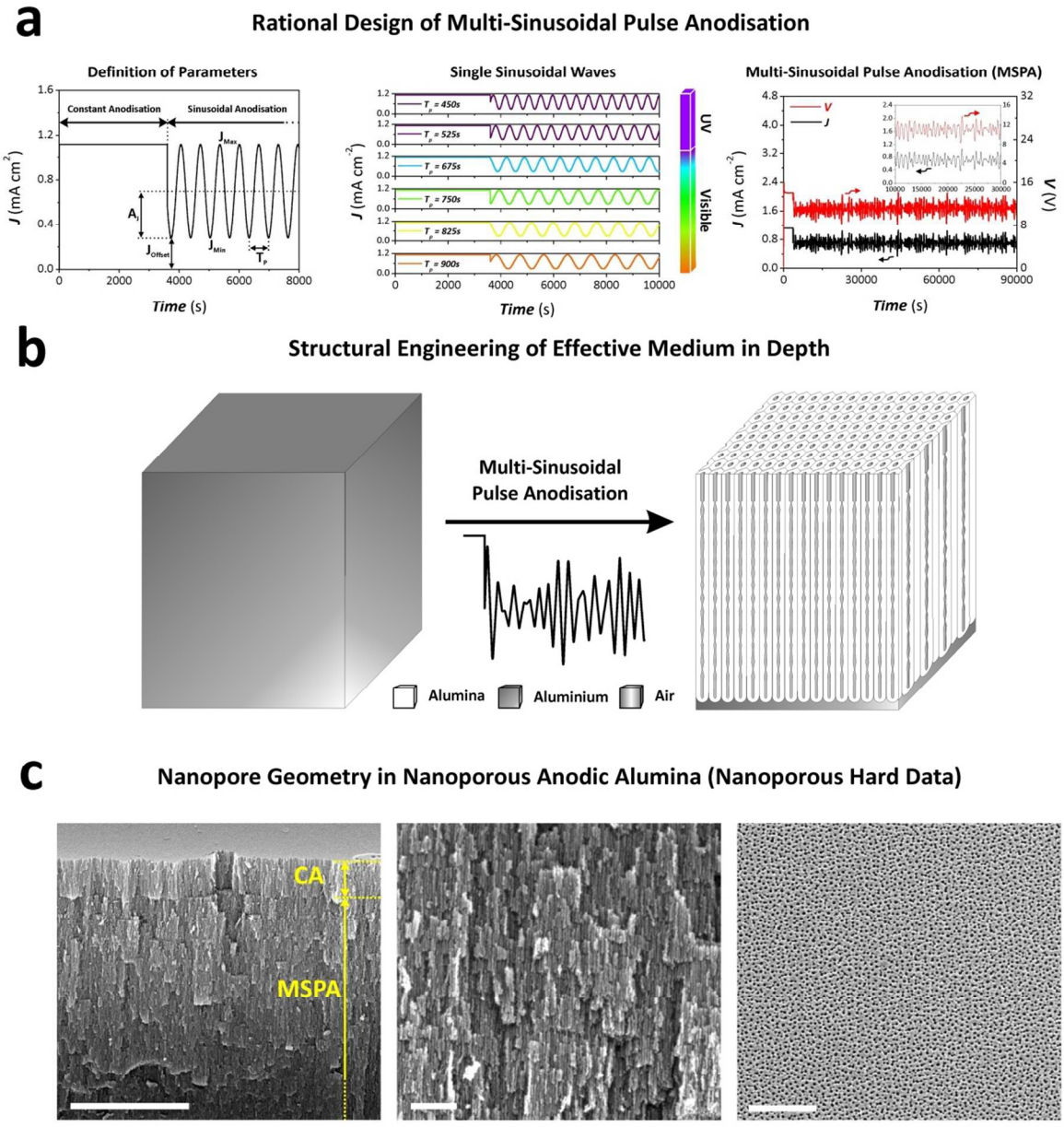

Fig. 1 Structural engineering of nanoporous anodic alumina photonic crystals by multi-sinusoidal pulse anodisation. a) Representative current density anodisation profiles used to encode information within the structure of nanoporous anodic alumina photonic crystals (from left to right: definition of anodisation parameters used to create single sinusoidal waves: A_J = anodisation amplitude, J_{Off} = anodisation offset, T_P = anodisation period, J_{Max} = current density maximum and J_{Min} = current density minimum; Multiple sinusoidal anodisation waveforms of different T_P; Multi-sinusoidal anodisation waveform resulting from the average sum of single sinusoidal waves – actual anodisation profile for code 01101111). b) Schematic illustration describing how the structure of NAA is engineered in depth by galvanostatic multi-sinusoidal pulse anodisation to create a NAA photonic crystal. c) Representative cross-section and top view SEM images of NAA produced by multi-sinusoidal pulse anodisation (scale bar (left) = 5 μm; scale bar (centre and right) = 500 nm) (NB: CA = constant anodisation and MSPA = multi-sinusoidal pulse anodisation).

Nanoscale Accepted Manuscript

 This journal is © The Royal Society of Chemistry 2012

View Article Online
DOI: 10.1039/C6NR01068G

Nanoscale

RSCPublishing

PAPER

Published on 14 March 2016. Downloaded by University of California - San Diego on 14/03/2016 13:36:14.

Herein, we present an innovative anodisation approach, so-called multi-sinusoidal pulse anodisation (MSPA), based on the combination of multiple sinusoidal waves into a single complex waveform, which corresponds to the average sum of several sinusoidal waves. This electrochemical nanofabrication method is demonstrated as a unique means of engineering the photonic stop band of nanoporous anodic alumina in depth. NAA photonic crystals produced by MSPA can be used to encode information within their optical transmission spectrum. As a proof-of-concept, a 8-bit encoding system with ON(1)/OFF(0) states is for the first time implemented and demonstrated in NAA-based photonic crystals, opening new opportunities for robust and reliable nanoscale platforms for secure information storage and optical encoding.

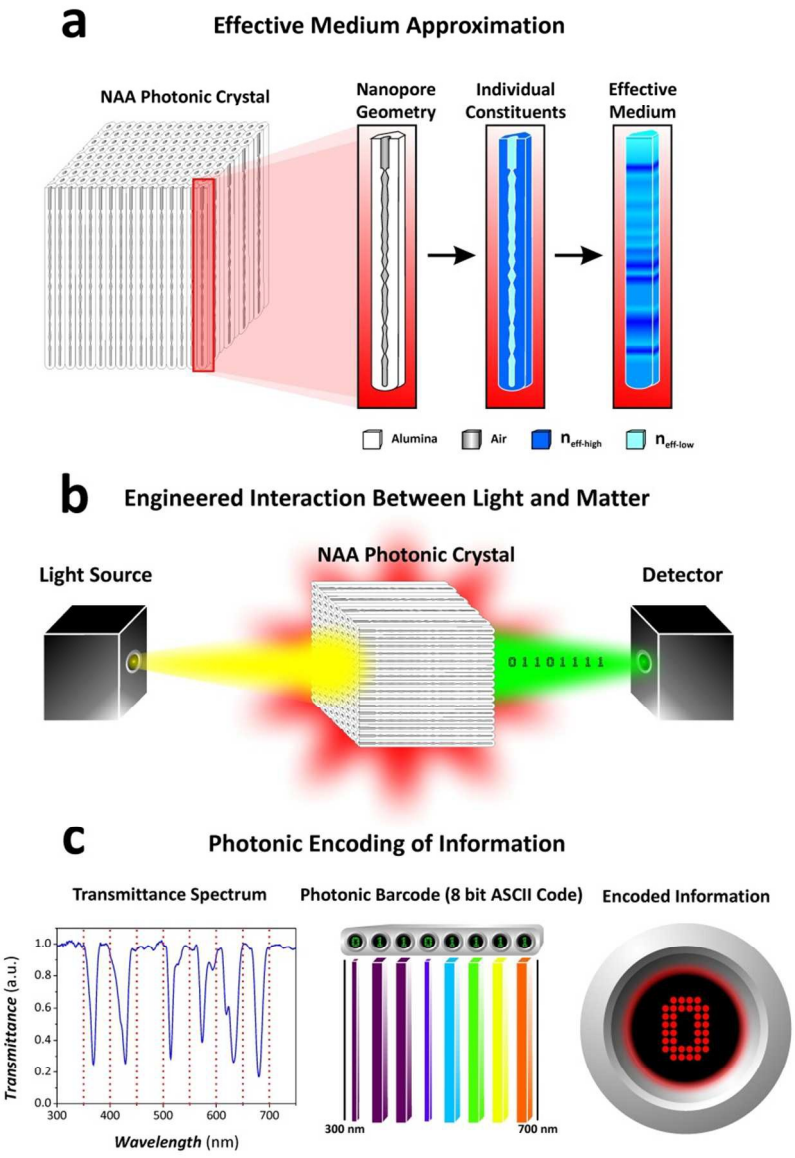

Fig. 2 Optical encoding of information within the spectral signature of nanoporous anodic alumina photonic crystals. a) Schematic illustration showing how the effective medium of nanoporous anodic alumina is engineered in depth by MSPA through changes in porosity (i.e. effective medium approximation). b) Scheme depicting how the interaction between light and matter can be engineered by creating NAA photonic crystals with precisely designed photonic stop band. c) Optical encoding of information within the transmittance spectrum of NAA photonic crystals and its conversion into photonic barcodes (example 01101111 = '*o*' in 8-bit ASCII system).

Nanoscale Accepted Manuscript

View Article Online
DOI: 10.1039/C6NR01068G

Nanoscale RSCPublishing

PAPER

Published on 14 March 2016. Downloaded by University of California - San Diego on 14/03/2016 13:36:14.

Results and discussion

Fabrication of NAA photonic crystals by multi-sinusoidal pulse anodisation

NAA photonic films were produced by anodisation of aluminium (Al) foils through a rationally designed multi-sinusoidal pulse anodisation approach under current density control in an aqueous solution 1.1 M sulfuric acid (H_2SO_4). In this study, the method employed to prepare these photonic crystals involves the generation of a current density-time anodisation waveform that can be precisely translated into changes of porosity/nanopore geometry in depth, as the nanoporous oxide layer grows. The algorithm used to encode information within the transmission spectrum of NAA photonic crystals is schematically described in **Fig. 1**. The multi-sinusoidal anodisation waveform used in the current study results from the superposition of n sine waves of different periods (**Fig. 1a**). According to our previous work, the current density for each individual sine wave is given by **Eq. 1**:[58]

$$J_i(t) = A_{J-i} \cdot \left[\mathrm{Sin}\left(\frac{2\pi}{T_{P-i}} \cdot t \right) + 1 \right] + J_{Off-i} \quad (1)$$

where $J_i(t)$ is the current density of the sinusoidal wave i at a given time t, A_{J-i} is the current density amplitude, T_{P-i} is the anodisation period and J_{Off-i} is the current density offset of that wave.

Therefore, the resulting multi-sinusoidal current density waveform (i.e. $J(t)$) is calculated as the average sum of the individual sinusoidal waves according to **Eq. 2**:

$$J(t) = \frac{\sum_{i=1}^{i=n} J_i(t)}{n} \quad (2)$$

Translation of anodisation profiles into optical encoding of information within NAA photonic crystals

In this study, the generated anodisation waves contain all the encoded information in the form of a 8-bit ASCII system, which is physically converted into a NAA photonic crystal platform by anodising aluminium through the aforementioned electrochemical process. It is worth noting that the anodisation conditions employed in our study make it possible to engineer the effective medium of NAA with precision, enabling the direct translation of these complex anodisation waves into changes of porosity/nanopore geometry (**Fig. 1b**). Anodisation under current density control provides a more accurate means of controlling the porosity and growth rate of NAA, which are critical parameters to create photonic crystals with precisely engineered photonic stop band. The resulting NAA photonic crystals feature a complex nanoporous structure from top to bottom (**Fig. 1c**). These nanoporous structures resemble photonic coatings present in natural organisms such as beetles and butterflies.[59] The porosity profile in depth displayed by these photonic structures corresponds directly with the multi-sinusoidal waveform used in the anodisation process (**Fig. 2a**).[10]

As far as the UV-visible transmission spectrum of these NAA photonic crystals is concerned (**Fig. 2b**), this features well-resolved transmission peaks, which correspond to the Fourier transform of the multi-sinusoidal waveform used in fabricating each of these NAA-based photonic crystals (**Fig. 2c**). The wavelengths at which these peaks are located within the UV-visible range can be precisely tuned by means of the anodisation profile, enabling the optical encoding of information within the spectroscopic signature of the NAA photonic crystal. In this system, any peak can be added or deleted from the spectrum by adding or removing the corresponding sinusoidal wave in **Eq. 2**. Furthermore, this binary system can also be converted into photonic barcodes (see **Fig. 2c**).[60] In the proposed barcode system, which can be approximated to that of the universal product code (UPC), the position and colour of each bar correspond to the wavelength at which the transmission peak is located and the width of these bars is associated with ON(1 = wide) and OFF(0 = thin) status, respectively. **Table 1** summarises the average positions and the full widths at half maximum (FWHM) of the different transmission peaks in the proposed 8-bit optical encoding system using NAA photonic platforms. These results confirm that MSPA is an effective nanofabrication method to engineer the effective medium of NAA in depth and to tune its transmission peaks across the UV-visible spectrum.

Demonstration of a 8-bit optical encoding system in NAA photonic crystals

In order to assess the feasibility of the proposed optical encoding system, eight multi-sinusoidal waveforms were generated according to **Eq. 2** and converted into NAA photonic crystals with unique photonic fingerprints. While the amplitude (A_{J-i}) and offset (J_{Off-i}) of the raw sinusoidal waves were each set to 0.420 mA cm^{-2} and 0.28 mA cm^{-2}, respectively, the anodisation period (T_{P-i}) was systematically modified (i.e. from 450 to 900 s with ΔT_{P-i} = 75 s) in order to generate up to seven equidistant peaks across the transmission spectrum of NAA photonic crystals (NB: the peak located at 375 s was set at OFF(0) throughout the experiments). **Table 1** summarises the anodisation period of the individual sinusoidal waves associated with the different peaks in the transmission spectrum of NAA photonic crystals. Therefore, a total of 256 codes can be readily implemented in the presented system (i.e. number of codes = $states^{bits} = 2^8 = 256$ codes).

Fig. 3 displays the single sinusoidal anodisation waves, the resulting anodisation profiles and scanning electron microscopy (SEM) cross-section view images of four representative NAA photonic crystals containing 8-bit ASCII codes generated by multi-sinusoidal waves combining 1, 3, 5 and 7 individual sinusoidal waves (i.e. ASCII codes 01000000, 01110000, 01111100 and 01111111). Cross-section SEM images of these photonic structures reveal that these NAA films are composed of stacks of nanoporous layers, the porosity, thickness and periodicity of which are correlated with the anodisation profile

Nanoscale Accepted Manuscript

Nanoscale View Article Online DOI: 10.1039/C6NR01068G PAPER

Published on 14 March 2016. Downloaded by University of California - San Diego on 14/03/2016 13:36:14.

used to fabricate them. Another unique feature of these photonic crystals is that they present characteristic interferometric colours (see digital pictures in **Fig. 3**) generated by the interaction light-matter. This property could be used as a fingerprint to identify encoded information by simple visualization.[54] The UV-visible transmission spectra and optical barcodes of the NAA photonic crystals displayed in **Fig. 3** are shown in **Fig. 4**. These results demonstrate that MSPA makes it possible to engineer the photonic stop band of NAA as so tune the transmission peaks at specific locations within the UV-visible spectrum. Finally, as a demonstration of the versatility and capability of these nanophotonic encoding platforms, **Figs. S1** and **S2** (**ESI**) summarise the anodisation profiles, SEM cross-section images, digital pictures, transmission spectra and photonic barcodes of NAA photonic crystals created by combining up to eight individual sinusoidal waves (i.e. ASCII codes 01000000, 01100000, 01110000, 01111000, 01111100, 01111110 and 01111111).

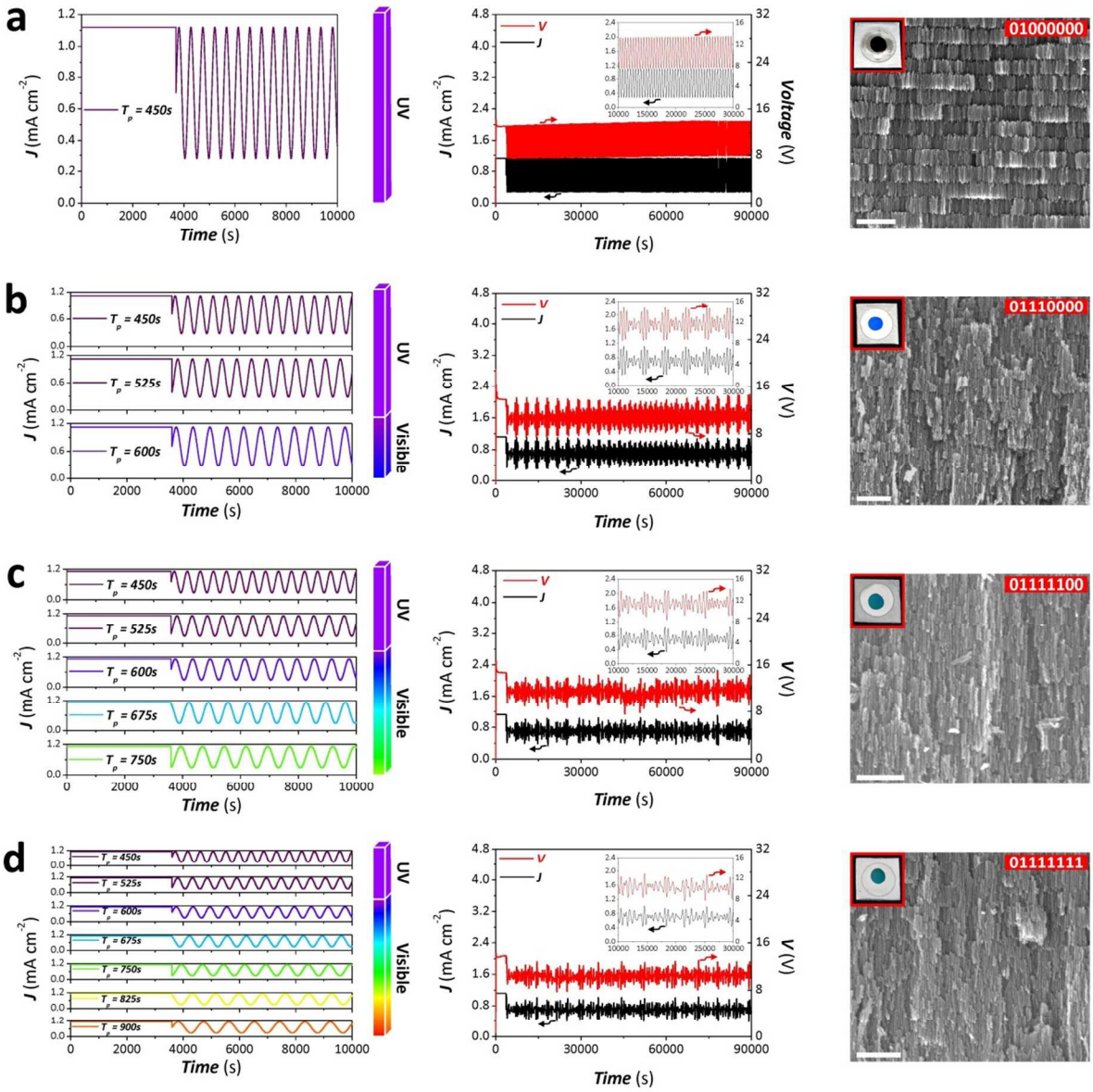

Fig. 3 Generation of a 8-bit ASCII encoding system in nanoporous anodic alumina photonic crystals by MSPA (scale bars = 500 nm). Single sinusoidal anodisation waves (left), actual anodisation profiles with resulting multi-sinusoidal waveforms (centre – inset showing magnified views of anodisation profiles) and cross-section SEM images of NAA photonic crystals (inset displays a digital picture of the resulting NAA photonic crystal) with codes: a) 01000000 (number of waves ON = 1 – T_p = 450s), b) 01110000 (number of waves ON = 3 – T_p = 450, 525 and 600s), c) 01111100 (number of waves ON = 5 – T_p = 450, 525, 600, 675 and 750s) and d) 01111111 (number of waves ON = 7 – T_p = 450, 525, 600, 675, 750, 825 and 900s).

Effective optical encoding of information within NAA photonic crystals

To demonstrate the capability of the proposed encoding 8-bit ASCII platform based on NAA photonic crystals, we first encoded the abbreviated name of our university (i.e. '*uoa*' – The University of Adelaide) into three different NAA photonic crystals, each of them containing one character encoded in 8-bit ASCII system (i.e. '*u*' = 01110101, '*o*' = 01101111 and '*a*' = 01100001). **Fig. 5** displays the anodisation profiles, SEM cross-section view images and digital pictures of these samples. Each of these NAA photonic crystals features a different

Nanoscale Accepted Manuscript

View Article Online
DOI: 10.1039/C6NR01068G

interferometric colour (i.e. '*u*' slightly purple, '*o*' dark yellow and '*a*' red). **Fig. 6** summarises the transmission spectra, the photonic barcodes and optical images of NAA photonic crystals containing the characters '*u*', '*o*' and '*a*'. The transmission spectrum of these photonic structures reveals well-resolved characteristic transmission peaks across the UV-visible spectrum, which correspond to the 8-bit ASCII codes of '*u*', '*o*' and '*a*'. These optical signals can be converted into photonic barcodes by the above-mentioned system. Furthermore, we observed that these photonic films keep the optical properties when they are broken down into micro-sized particles, as revealed by optical images.[54]

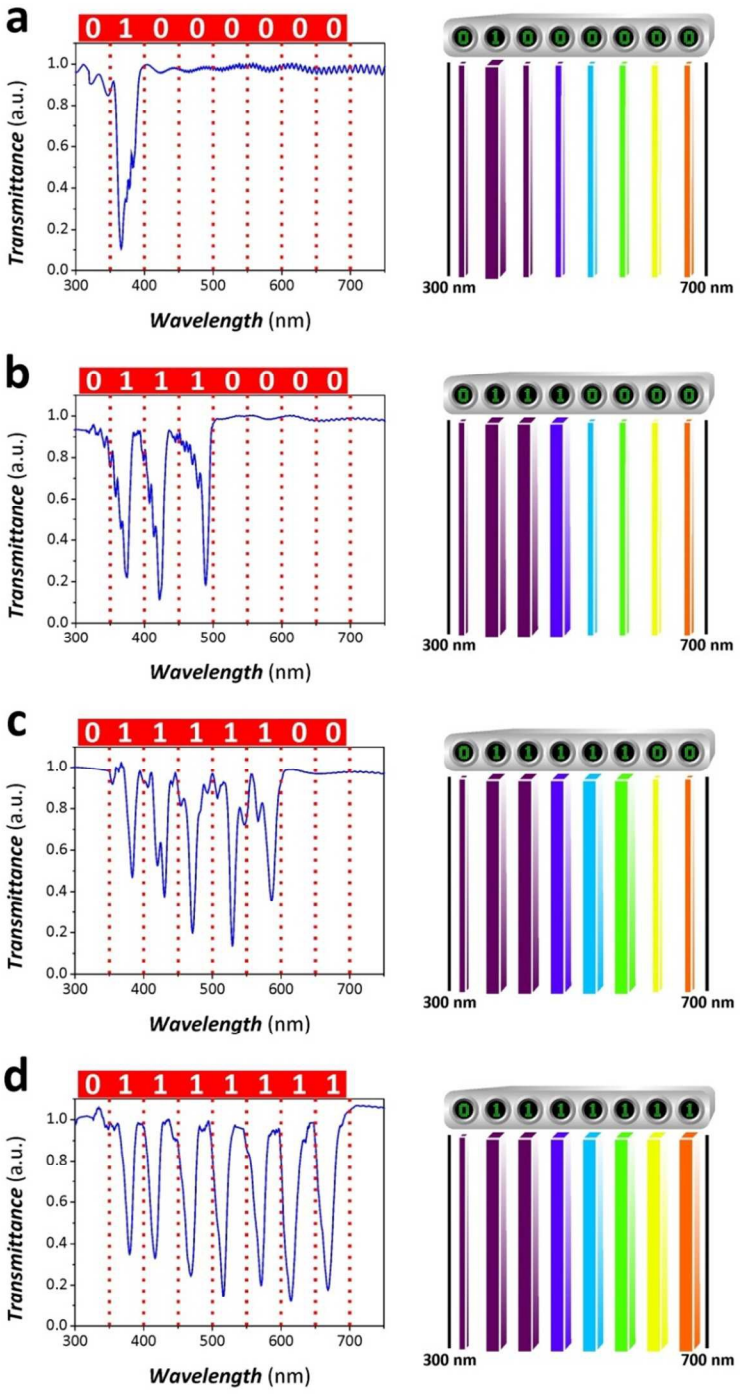

Fig. 4 Optical encoding of information within the transmission spectrum of nanoporous anodic alumina photonic crystals. a) Transmission spectrum and photonic barcode of a NAA photonic crystal with code: 01000000 (number of waves ON = 1 – T_p = 450s). b) Transmission spectrum and photonic barcode of a NAA photonic crystal with code: 01110000 (number of waves ON = 3 – T_p = 450, 525 and 600s). c) Transmission spectrum and photonic barcode of a NAA photonic crystal with code: 01111100 (number of waves ON = 5 – T_p = 450, 525, 600, 675 and 750s). c) Transmission spectrum and photonic barcode of a NAA photonic crystal with code: 01111111 (number of waves ON = 7 – T_p = 450, 525, 600, 675, 750, 825 and 900s).

Published on 14 March 2016. Downloaded by University of California - San Diego on 14/03/2016 13:36:14.

Nanoscale Accepted Manuscript

This journal is © The Royal Society of Chemistry 2012

View Article Online
DOI: 10.1039/C6NR01068G

Nanoscale

RSCPublishing

PAPER

Published on 14 March 2016. Downloaded by University of California - San Diego on 14/03/2016 13:36:14.

Finally, as a proof-of-concept, we proved the full capability of this system by optically encoding the string '*the university of adelaide*' in a set of NAA photonic crystals. **Fig. 7** shows the digital pictures and codes of these photonic crystals, the anodisation profiles, transmission spectra, photonic barcodes, raw sinusoidal waves and ASCII codes of which are summarised in **Fig. S3** and **Table S1** (**ESI**). As this figure reveals, each of these NAA photonic crystals features a unique spectroscopic signature in the form of UV-visible transmission spectra, photonic barcodes and interferometric colours.

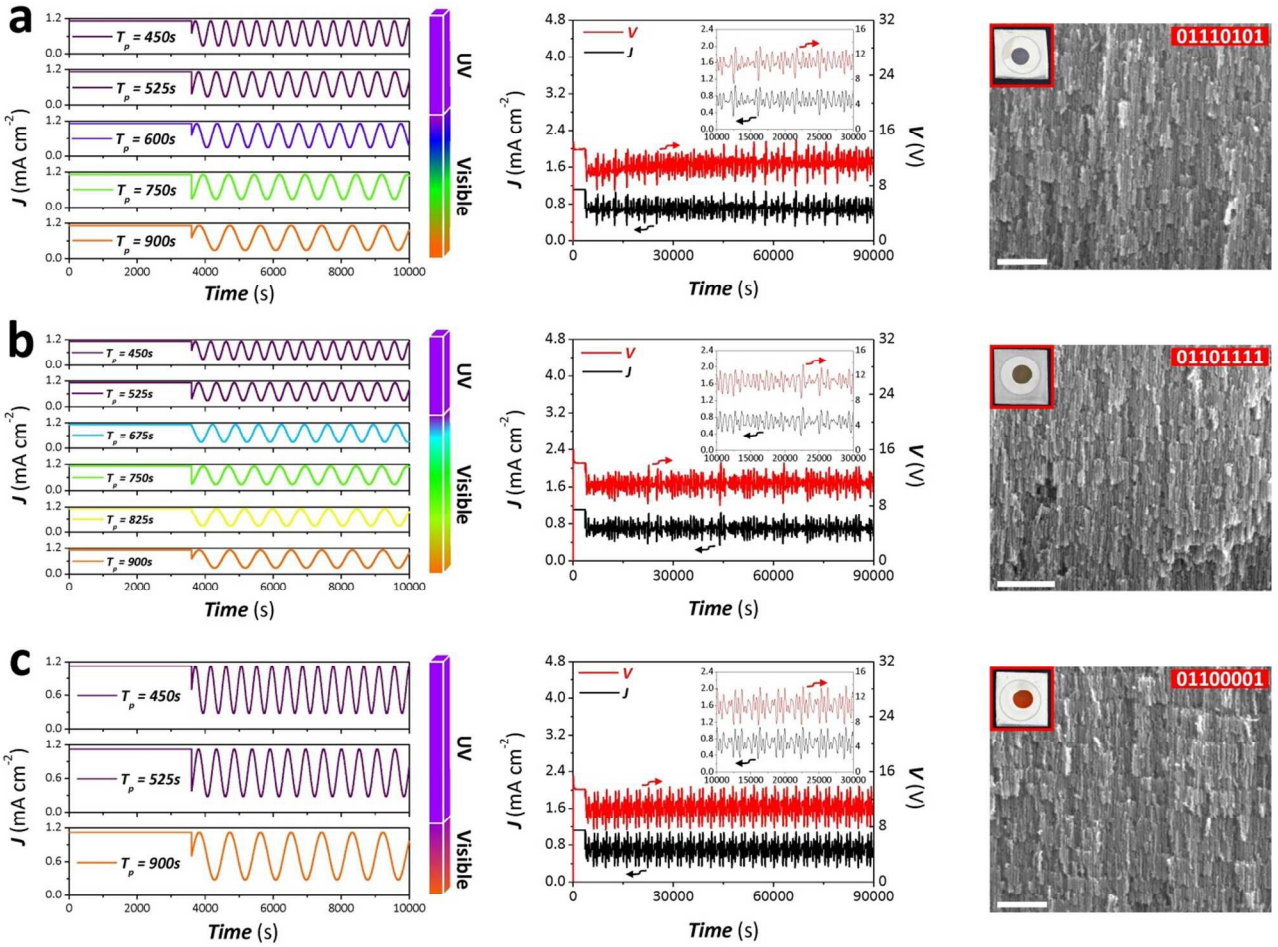

Fig. 5 Optical encoding of the string '*uoa*' using a 8-bit ASCII code within nanoporous anodic alumina photonic crystals by MSPA (scale bars = 500 nm). a) Single sinusoidal anodisation waves (left), anodisation profile with resulting multi-sinusoidal waveform (centre – inset showing magnified view) and cross-section view SEM image of a NAA photonic crystal with code: 01110101 = '*u*' (number of waves ON = 5 – T_p = 450, 525, 600, 750 and 900s) (inset displays a digital picture of the resulting NAA photonic crystal). b) Single sinusoidal anodisation waves (left), anodisation profile with resulting multi-sinusoidal waveform (centre – inset showing magnified view) and cross-section view SEM image of a NAA photonic crystal with code: 01101111 = '*o*' (number of waves ON = 6 – T_p = 450, 525, 675, 750, 825 and 900s) (inset displays a digital picture of the resulting NAA photonic crystal). c) Single sinusoidal anodisation waves (left), anodisation profile with resulting multi-sinusoidal waveform (centre – inset showing magnified view) and cross-section view SEM image of a NAA photonic crystal with code: 01100001 = '*a*' (number of waves ON = 3 – T_p = 450, 525 and 900s) (inset displays a digital picture of the resulting NAA photonic crystal).

Conclusions

In this study, we have demonstrated for the first time the capability and versatility of NAA photonic crystals to store encoded information in the form of a 8-bit ASCII system based on the tuneability of the characteristic transmission peaks of NAA across the UV-visible spectrum. A rationally designed multi-sinusoidal pulse anodisation approach performed under specific conditions can be used to engineer the effective medium of NAA in depth with precision. So, information can be encoded within the spectroscopic signature of the resulting NAA-based photonic crystals. This robust method has been

Nanoscale Accepted Manuscript

PAPER View Article Online DOI: 10.1039/C6NR01068G Nanoscale

Published on 14 March 2016. Downloaded by University of California - San Diego on 14/03/2016 13:36:14.

demonstrated considering two states (i.e. ON(1) and OFF(0)) per bit in a 8-bit ASCII system, with the capability to create a total of 256 different codes. Furthermore, we have proposed a new barcode system based on the transmission spectrum of NAA photonic crystals as a means of information encoding. In these 'photonic barcodes' the position and colour of each bar correspond to the wavelength at which the transmission peak is located within the transmission spectrum of NAA photonic crystals and the width of these bars is associated with ON(1 = wide) and OFF(0 = thin) status, respectively.

Although the number of codes that can be generated by this system is limited (i.e. 256), it is expected that this new anodisation approaches will make it possible to implement more sophisticated optical encoding approaches able to store a higher number of codes and complex information within NAA photonic crystals. Furthermore, these NAA-based photonic crystals can be broken down into micro-sized particles, which could be readily used for high throughput label-free molecular screening and sensing applications, encoding platforms of information as photonic tags and tracers and self-reporting drug releasing micro-sized containers.

Finally, as a proof-of concept, we have encoded the string of characters '*the university of adelaide*' in a set of NAA photonic crystals, demonstrating the potential of this system for optical encoding of information in a robust and chemically stable nanoscale photonic platform.

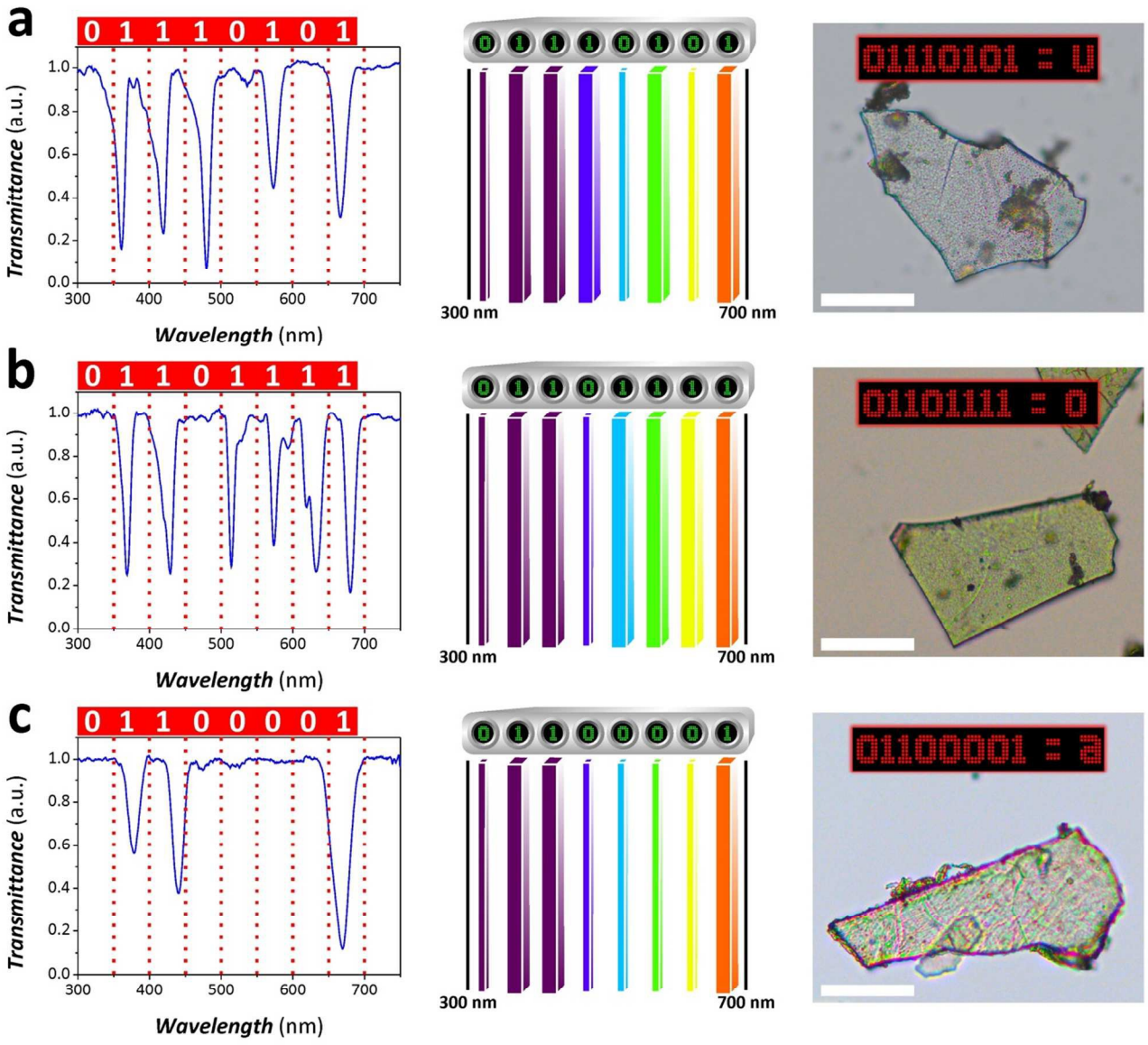

Fig. 6 Optical encoding of the string '*uoa*' within the transmission spectrum of nanoporous anodic alumina photonic crystals (scale bars = 100 μm). a) Transmission spectrum, photonic barcode and optical microscope image of a NAA photonic crystal with code: 01110101 = '*u*' (number of waves ON = 5 – T_p = 450, 525, 600, 750 and 900s). b) Transmission spectrum, photonic barcode and optical microscope image of a NAA photonic crystal with code: 01101111 = '*o*' (number of waves ON = 6 – T_p = 450, 525, 675, 750, 825 and 900s). c) Transmission spectrum, photonic barcode and optical microscope image of a NAA photonic crystal with code: 01100001 = '*a*' (number of waves ON = 3 – T_p = 450, 525 and 900s).

Nanoscale Accepted Manuscript

 This journal is © The Royal Society of Chemistry 2012

View Article Online
DOI: 10.1039/C6NR01068G

Nanoscale

RSCPublishing

PAPER

Published on 14 March 2016. Downloaded by University of California - San Diego on 14/03/2016 13:36:14.

Experimental

Materials

High purity aluminium (Al) foils (99.9997%) 0.32 mm thick were supplied by Goodfellow Cambridge Ltd. (UK). Sulphuric acid (H_2SO_4), perchloric acid ($HClO_4$), phosphoric acid (H_3PO_4), hydrochloric acid (HCl), cupric chloride ($CuCl_2$) and ethanol (C_2H_5OH – EtOH) were purchased from Sigma-Aldrich (Australia) and used as-received, without further purification. All the aqueous solutions used in this study were prepared using ultrapure water Option Q–Purelabs (Australia).

Fabrication of NAA photonic crystals

NAA photonic films were produced by anodisation of Al foils through a rationally designed pulse anodisation approach. This process was performed under current density control in an aqueous solution 1.1 M sulfuric acid (H_2SO_4). Prior to anodization, 1.5 x 1.5 cm square Al substrates were cleaned under ultra-sonication in ethanol (EtOH) and ultrapure water for 15 min each. Then, Al substrates were electropolished in a mixture of EtOH and $HClO_4$ 4:1 (*v*:*v*) at 20 V and 5^{0}C for 3 min. The anodisation process was performed in a single step, which started by applying constant current density of 1.12 mA cm^{-2} for 1 h at -1^{0}C in order to create a thin nanoporous oxide layer. This initial layer acted as a shuttle to achieve a homogeneous pore growth prior to sinusoidal anodisation.

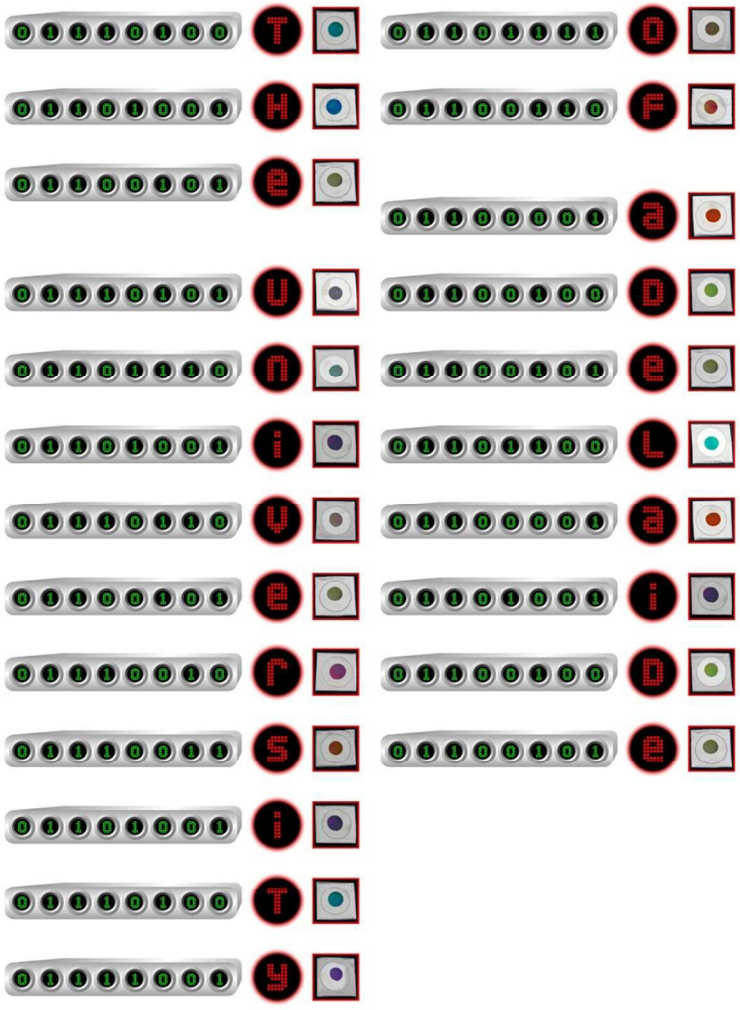

Fig. 7 Optical encoding of the string '*the university of adelaide*' within nanoporous anodic alumina photonic crystals produced by multi-sinusoidal pulse anodisation. Details showing the 8-bit ASCII code corresponding to each character and digital pictures of NAA photonic crystals when that character has been optically encoded.

Nanoscale Accepted Manuscript

View Article Online
DOI: 10.1039/C6NR01068G

Nanoscale RSCPublishing

PAPER

Published on 14 March 2016. Downloaded by University of California - San Diego on 14/03/2016 13:36:14.

Note that 25 *v*% of EtOH was added to the electrolyte solution to prevent it from freezing at temperatures below 0^0C.[61-63] After this, the anodisation profile was set to multi-sinusoidal pulse mode, in the course of which the anodisation current density was sinusoidally pulsed according to the resulting anodisation waveform obtained from **Eq. 2**. The different current density-time anodisation waveforms used to produce of NAA photonic crystals were automatically created by a custom-designed Labview®-based software. The anodisation process was carried out in a custom-built anodisation cell equipped with thermostat control in order to keep the electrolyte temperature constant throughout anodisation and mechanical stirring. A final pore widening step in an aqueous solution 5 *wt*% H_3PO_4 at 35°C for 8 min was applied to all nanoporous anodic alumina photonic crystals.

Table 1. Anodisation period, UV-visible range, position and FWHM of the characteristic transmission peaks created in nanoporous anodic alumina photonic crystals by multi-sinusoidal pulse anodisation for a 8-bit ASCII system.

T_p (s)	Range	Peak Position (nm)	Peak FWHM
450	350-400 nm	369 ± 5	15 ± 3
525	400-450 nm	425 ± 7	17 ± 4
600	450-500 nm	477 ± 6	15 ± 3
675	500-550 nm	523 ± 6	15 ± 4
750	550-600 nm	573 ± 7	17 ± 8
825	600-650 nm	627 ± 6	19 ± 6
900	650-700 nm	672 ± 6	21 ± 6

Optical characterisation of NAA photonic crystals

UV-visible spectra of NAA photonic crystals were acquired using a UV-visible spectrometer (Cary 60, Agilent, USA) from 300 to 800 nm with a resolution of 1 nm. Note that the remaining aluminium substrate of NAA photonic crystals was dissolved by selective wet chemical etching in a saturated solution of $HCl/CuCl_2$ through an etching mask with a circular window of 5 mm in diameter. Digital images of NAA photonic crystals were acquired by a Sony HX90V Compact Camera with 18.2 MP and 30x optical zoom and autofocus function under natural illumination. Micro-sized NAA photonic crystals were characterised by an optical microscope (Nikon LV100 POL optical petrographic microscope).

Structural characterisation

The nanoporous structure of NAA photonic crystals was characterised by field emission gun scanning electron microscopy (FEG-SEM FEI Quanta 450).

Acknowledgements

Authors acknowledge the support provided by the Australian Research Council (ARC) through the grants number DE140100549, DP120101680 and FT110100711 and the School of Chemical Engineering (UoA). Authors also thank the Adelaide Microscopy (AM) centre for FEG-SEM characterization.

Notes and references

[1]School of Chemical Engineering, The University of Adelaide, Engineering North Building, 5005 Adelaide, Australia.
*E-mails: abel.santos@adelaide.edu.au ; dusan.losic@adelaide.edu.au

Dr. Abel Santos conceived the idea, designed and carried out the experimental part of this work assisted by Cheryl Suwen Law and Taj Pereira. The obtained results were discussed and analysed by all the authors. The final version of the manuscript was written through contributions of all the authors. All the authors have given their approval to the final version of the manuscript.

Electronic Supplementary Information (ESI) available: The Supporting Information file provides further details about anodization profiles, SEM cross-section images, digital pictures, transmission spectra, photonic barcodes and ASCII codes of the different NAA photonic crystals fabricated and analysed in our study. Supporting Information is available from the Wiley Online Library or from the author. See DOI: 10.1039/b000000x/

1 M. McCulloch, S. Fallon, T. Wyndham, E. Hendy, J. Lough and D. Barnes, *Nature* 2003, **421**, 727-730.

2 D. J. Barnes and J. M. Lough, *GCB Bioenergy* 1996, **2**, 569-582.

3 J. A. Ferguson, T. C. Boles, C. P. Adams and D. R. Walt, *Nat. Biotechnol.* 1996, **14**, 1681-1684.

4 J. Yoon, *Angew. Chem. Int. Ed.* 2014, **53**, 6600-6601.

5 M. Jr. Bruchez, M. Moronne, P. Gin, S. Weiss and A. P. Alivisatos, *Science* 1998, **281**, 2013-2016.

6 H. Fenniri, L. Ding, A. E. Ribbe and Y. Zyrianov, *J. Am. Chem. Soc.* 2001, **123**, 8151-8152.

7 W. C. Chan and S. Nie, *Science* 1998, **281**, 2016-2018.

8 S. R. Nicewarner-Peña, R. G. Freeman, B. D. Reiss, L. He, D. J. Peña, I. D. Walton, R. Cromer, C. D. Keating and M. J. Natan, *Science* 2001, **294**, 137-141.

9 F. Cunin, T. A. Schemedake, J. R. Link, Y. Y. Li, J. Koh, S. N. Bhatia and M. J. Sailor, *Nat. Mater.* 2002, **1**, 39-41.

10 S. O. Meade, M. S. Yoon, K. H. Ahn and M. J. Sailor, *Adv. Mater.* 2004, **16**, 1811-1814.

Nanoscale Accepted Manuscript

Nanoscale View Article Online DOI: 10.1039/C6NR01068G PAPER

Published on 14 March 2016. Downloaded by University of California - San Diego on 14/03/2016 13:36:14.

11 M. G. Berger, R. Arens-Fisher, M. Thönissen, M. Krüger, S. Billat, H. Lüth, S. Hilbrich, W. Theiβ and P. Grosse, *Thin Solid Films* 1997, **297**, 237-240.

12 S. O. Meade and M. J. Sailor, *Phys. Stat. Sol. (RRL)* 2007, **1**, R71-R73.

13 M. Y. Chen, S. O. Meade and M. J. Sailor, *Phys. Stat. Sol. C* 2009, **6**, 1610-1614.

14 S. O. Meade, M. Y. Chen, M. J. Sailor and G. M. Miskelly, *Anal. Chem.* 2009, **81**, 2618-2625.

15 Y. Y. Li, F. Cunin, J. R. Link, T. Gao, R. E. Betts, S. H. Reiver, V. Chin, S. N. Bhatia and M. J. Sailor, *Science* 2003, **299**, 2045-2047.

16 T. Jalkanen, E. Mäkilä, Y. –I. Suzuki, T. Urata, K. Fukami, T. Sakka, J. Salonen and Y. H. Ogata, *Adv. Funct. Mater.* 2012, **22**, 3890-3898.

17 S. Ciampi, J. B. Harper and J. J. Gooding, *Chem. Soc. Rev.* 2010, **39**, 2158-2183.

18 W. Lee and W. J. S. Park, *Chem. Rev.* 2014, **114**, 7487-7556.

19 H. Masuda and F. Fukuda, *Science* 1995, **268**, 1466-1468.

20 H. Masuda and F. J. Hasegwa, *J. Electrochem. Soc.* 1997, **144**, L127-L130.

21 H. Masuda, K. Yada and A. Osaka, *Jpn. J. Appl. Phys.* 1998, **37**, L 1340-L 1342.

22 K. Nielsch, J. Choi, K. Schwirn, R. B. Wehspohn and U. Gösele, *Nano Lett.* 2002, **2**, 677-680.

23 W. Cheng, M. Steinhart, U. Gösele and R. B. Wehrspohn, *J. Mater. Chem.* 2007, **17**, 3493-3495.

24 W. Lee and J. C. Kim, *Nanotechnology* 2010, **21**, 485304.

25 A. Santos, J. M. Montero-Moreno, J. Bachmann, K. Nielsch, P. Formentín, J. Ferré-Borrull, J. Pallarès and L. F. Marsal, *ACS Appl. Mater. Interfaces* 2011, **3**, 1925-1932.

26 W. Lee, R. Ji, U. Gösele and K. Nielsch, *Nat. Mater.* 2006, **5**, 741-747.

27 K. Schwirn, W. Lee, R. Hillebrand, M. Steinhart, K. Nielsch and U. Gösele, *ACS Nano* 2008, **2**, 302-310.

28 W. Lee, K. Schwirn, M. Steinhart, E. Pippel, R. Scholz and U. Gösele, *Nat. Nanotechnol.* 2008, **3**, 234-239.

29 W. Lee, J. C. Kim and U. Gösele, *Adv. Funct. Mater.* 2010, **20**, 21-27.

30 W. Lee, R. Scholz and U. Gösele, *Nano Lett.* 2008, **8**, 2155-2160.

31 T. Kumeria, M. M. Rahman, A. Santos, J. Ferré-Borrull, L. F. Marsal and D. Losic, *Anal. Chem.* 2014, **86**, 1837-1844.

32 T. Kumeria, M. M. Rahman, A. Santos, J. Ferré-Borrull, L. F. Marsal and D. Losic, *ACS Appl. Mater. Interfaces* 2014, **6**, 12971-12978.

33 T. Kumeria, A. Santos, M. M. Rahman, J. Ferré-Borrull, L. F. Marsal and D. Losic, *ACS Photonics* 2014, 1, 1298-1306.

34 A. Santos, T. Kumeria and D. Losic, D. *Materials* 2014, **7**, 4297-4320.

35 T. Kumeria, A. Santos and D. Losic, *Sensors* 2014, **14**, 11878-11918.

36 A. Santos, T. Kumeria and D. Losic, D. *TrAC, Trends Anal. Chem.* 2013, **44**, 25-38.

37 A. Santos, T. Kumeria, Y. Wang and D. Losic, *Nanoscale* 2014, **6**, 9991-9999.

38 A. Santos, V. S. Balderrama, M. Alba, P. Formentín, J. Ferré-Borrull, J. Pallarès and L. F. Marsal, *Adv. Mater.* 2012, **24**, 1050-1054.

39 Y. Chen, A. Santos, D. Ho, Y. Wang, T. Kumeria, J. Li, C. Wang and D. Losic, *Electrochim. Acta* 2015, **174**, 672-681.

40 Y. Wang, Y. Chen, T. Kumeria, F. Ding, A. Evdokiou, D. Losic and A. Santos. *ACS Appl. Mater. Interfaces* 2015, **7**, 9879-9888.

41 A. Santos, T. Kumeria and D. Losic, *Anal. Chem.* 2013, **85**, 7904-7911.

42 G. Macias, J. Ferré-Borrull, J. Pallarès and L.F. Marsal, *Nanoscale Res. Lett.* 2014, **9**, 315.

43 G. Macias, L. P. Hernández-Eguía, J. Ferré-Borrull, J. Pallarés and L.F. Marsal, *ACS Appl. Mater. Interfaces* 2013, **5**, 8093-8098.

44 W. J. Zheng, G. T. Fei, B. Wang, Z. Jin and L. D. Zhang, *Mater. Lett.* 2009, **63**, 706-708.

45 Q. Xu, H. Y. Sun, Y. H. Yang, L. H. Liu and Z. Y. Li, *Appl. Surf. Sci.* 2011, **258**, 1826-1830.

46 Y. Liu, H. H. Wang, J. E. Indacochea and M. L. Wang, *Sens. Actuators, B* 2011, **160**, 1149-1158.

47 G. L. Shang, G. T. Fei, Y. Zhang, P. Yan, S. H. Xu and L. D. Zhang, *J. Mater. Chem. C* 2013, **1**, 5285-5291.

48 B. Wang, G. T. Fei, M. Wang, M. G. Kong and L. D. Zhang, *Nanotechnology* 2007, **18**, 365601.

49 Y. Chen, A. Santos, Y. Wang, T. Kumeria, C. Wang, J. Li and D. Losic, *Nanoscale* 2015, **7**, 7770-7779.

50 A. Santos, G. Macias, J. Ferré-Borrull, J. Pallarés and L. F. Marsal, *ACS Appl. Mater. Interfaces* 2012, **4**, 3584-3588.

51 A. Santos, V. S. Balderrama, M. Alba, P. Formentín, J. Ferré-Borrull, J. Pallarès and L. F. Marsal, *Nanoscale Res. Lett.* 2012, **7**, 370.

52 T. Kumeria, A. Santos and D. Losic, *ACS Appl. Mater. Interfaces* 2013, **5**, 11783-11790.

53 Y. Chen, A. Santos, Y. Wang, T. Kumeria, J. Li, C. Wang and D. Losic, *ACS Appl. Mater. Interfaces* 2015, **7**, 19816-19824.

54 Y. Chen, A. Santos, Y. Wang, T. Kumeria, D. Ho, J. Li, C. Wang and D. Losic, *Sci. Rep.* 2015, **5**, 12893.

55 J. Martín, M. Martín-González, J. F. Fernández and O. Caballero-Calero, *Nat. Commun.* 2014, **5**, 5130.

56 D. Losic, M. Lillo and D. Jr. Losic, *Small* 2009, **5**, 12, 1392-1397.

57 D. Losic and D. Jr. Losic, *Langmuir* 2009, **25**, 5426-5431.

58 A. Santos, J. Yoo, C. V. Rohatgi, T. Kumeria, Y. Wang and D. Losic, *Nanoscale* 2016, 8, 1360-1373.

59 T. Ishizaki and M. Sakamoto, *Langmuir* 2011, **27**, 2375-2381.

60 R. C. Palmer in *The Bar Code Book: Reading, Printing, and Specification of Bar Code Symbols*, Bloomington, USA **2007**.

61 Z. Yao, M. Zheng, L. Ma and W. Shen, *Nanotechnology* 2008, **19**, 465705.

62 A. Santos, P. Formentín, J. Ferré-Borrull, J. Pallarès and L. F. Marsal, *Mater. Lett.* 2012, **67**, 296-299.

63 Y. Wang, A. Santos and A. Evdokiou, D. Losic, *Electrochim. Acta* 2015, **154**, 379-386.

Nanoscale Accepted Manuscript